Machine Learning Algorithm to Predict Cardiac Output Using Arterial Pressure Waveform Analysis

Liao Ke
School of Information Science
[1]*Japan Advanced Institute of Science and Technology*
[2]*Ricoh Software Research Center (Beijing) Co., Ltd.*
Nomi, Ishikawa, Japan
Ke.Liao@cn.ricoh.com

Xiao Wei
Xuanwu Hospital
Capital Medical University
Beijing, China
xiaowei@xwhosp.org

Wang Wei
Ricoh Software Research Center (Beijing) Co., Ltd.
Beijing, China
wei.wang5@cn.ricoh.com

Armagan Elibol
School of Information Science
Japan Advanced Institute of Science and Technology
Nomi, Ishikawa, Japan
aelibol@jaist.ac.jp

Liao Cenyu
School of Mathematical Science
Beijing Normal University
Beijing, China
202021130094@bnu.edu.cn

Nak Young Chong
School of Information Science
Japan Advanced Institute of Science and Technology
Nomi, Ishikawa, Japan
nakyoung@jaist.ac.jp

***Abstract*—Cardiac Output (CO) is a key hemodynamic variable that can be estimated in a minimally invasive way via using Arterial Pressure Waveform Analysis (APWA). Many models use circulation mechanics to build the relationship between arterial pressure and CO. In this study, we attempt to apply machine learning and feature engineering to analyze the Arterial Pressure Waveform (APW) and create regression models to predict the CO. We utilize the traditional APWA model knowledge and the time-domain, frequency-domain, and other characteristics of time series data for feature engineering. We present the benchmarking results for several machine learning models using the MIMIC-II waveform database. We compare the predicted CO values from our proposed models with the "gold standard" TCO (CO measured by intermittent pulmonary artery thermodilution). Our results show that the Random forest model has the most accurate agreement (MSE: 1.421 L/min, bias: -0.01 L/min, 95% limits of agreement: -2.35 L/min to +2.32 L/min, percentage error: 39.44%). Notably, the XGBoost model demonstrates good tracking ability with TCO (radius bias: 11.79°, 95% radius limits of agreement: ± 28.89°), achieving the clinically acceptable level.**

***Index Terms*—Cardiac Output, feature engineering, machine learning, Arterial Pressure Waveform**

I. Introduction

Hemodynamic monitoring plays an important role in perioperative and critical care. CO, a key hemodynamic variable, acts as a valuable tool for the diagnosis and management of critically ill patients [1]. Several ways have been presented in order to measure or estimate CO values. The Fick principle, as the first method to measure CO, was proposed in 1870 by Adolf Eugen Fick [2], using oxygen as the marker to calculate CO through the whole body's blood flow. Indicator dilution techniques are based on injecting a substance into the circulatory system and measuring its change in concentration over time, which relates to the rate of flow in the system. The substance could be Lithium [3] or cold saline (also called "Thermodilution", the gold standard methods in CO measurement and the measured CO is named TCO) [4].

As the indicator dilution techniques are invasive, minimally invasive or non-invasive methods are developed. APWA is widely used for estimating hemodynamic parameters. One of the most classical models is the "Windlessel model", proposed by Otto Frank [5] in 1899. It describes the elasticity or compliance of the large arteries as a pneumatic air chamber with the first-element model. Afterward, the extensions to two-element, three-element, and four-element models were proposed, considering more sophisticated factors, such as arterial impedance and oscillatory phenomenon. Becides, some models focused on finding the relationship between power and flow [6]. In contrast, others considered the waveform morphology [7]. All the aforementioned models are based on physical or mathematical modeling for the relationship between the blood flow, blood pressure, and power to estimate the CO, which is sophisticated and requires large-scale experiments for calibration and obtaining correction factors [8].

Recently, more advanced time series or waveform analysis models were introduced to analyze the hemodynamic parameters. Yang et al. [9] used deep learning models to extract the

characteristics of blood pressure waveform to estimate the CO. Moon et al. [10] presented a deep learning model to estimate SV (Stroke Volume, SV $\times$ HR (Heart Rate) = CO). Kwon et al. [11] estimate SVV (Stroke Volume Variance) from APW based on 1-D CNN (Convolutional Neural Network). This kind of research entails time and effort-intensive data collection, especially the TCO records to be served as a ground truth, which is difficult to collect as it requires invasive procedures.

In this work, we attempt to use the feature engineering and machine learning methods to estimate CO based on ABPW, without the need for collecting massive amounts of data. Specifically, we propose to fuse Hemodynamic, Waveform, and Demographic features and use regression-based machine learning models to estimate CO values. Furthermore, we conduct a benchmark testing of several machine learning models for the CO predicting task. We use the public MIMIC-II (Medical Information Mart for Intensive Care II) waveform dataset [12]. Our results indicate that machine learning models, especially Random forest and CatBoost, outperform other traditional APWA models [13] both in agreement and trending ability. Notably, XGBoost reaches the clinical requirement of trending tracking as defined in [14].

The rest of the paper is organized as follows: Data preprocessing procedures are outlined in the next section. Section III is devoted to the feature extraction procedures. Section IV details the results obtained using tested machine learning models and computational analysis. The last two sections are for Discussions and Conclusions, respectively.

II. Data Preparation

A. Datasets

Our dataset is extracted from the MIMIC-II Waveform Database Matched Subset [12], [15]. It contains $4,897$ waveform records and $5,266$ numeric records from bedside patient monitors in intensive care units (ICUs) of the MIMIC-II Waveform Database, which have been matched and time-aligned with $2,809$ MIMIC-II Clinical Database records [16]. Waveform records include one or more ECG (Electrocardiogram), ABP, PPG (Fingertip Photoplethysmogram), etc. Numeric records include HR, SpO2 (Oxygen saturation), SBP (systolic blood pressures), MAP (mean blood pressures), and DBP (diastolic blood pressures), TCO, etc. The database also records demographic and clinical information, including age, sex, ICD9 codes (Diagnostic Code Descriptions), Hematocrit (mean and standard), and medications.

B. Data segmentation

In the dataset, the ABP signals, sampled at 125 Hz, and the reference TCO measurements occur at irregular intervals. We extracted the ABP waveform and TCO measurement to compose the input segmentations. One segmentation contains the TCO at T_0 and ABP waveform with a time window of 10 seconds (T_{0-10S}, T_0), as shown in Fig. 1.

Mechanical ventilation results in a cyclical increase (during inspiration) and decrease (during expiration) of intra-thoracic pressures and these pressure fluctuations, in turn, alter the diastolic filling of the right and left ventricles. Therefore, we use the 10 seconds time window, which is based on the normal respiration rate to decrease the influence of the period of respiration on hemodynamic data [10], [17].

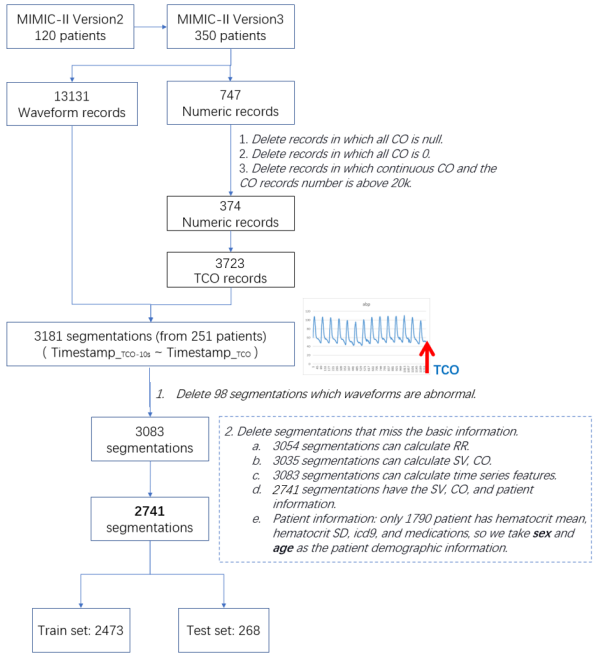

Fig. 1. The flowchart for data segmentation procedure.

III. Feature Engineering

Feature engineering is to extract features from ABP waveforms and demographic records. Fig. 2 shows the three types of features: 1) the features with hemodynamic meanings, extracted from the traditional ABPW models; 2) the features with waveform meanings, extracted based on the basic waveform or time series methods; 3) the demographic information with the standardization process. In total, 68 features forms the input vector for the machine learning models.

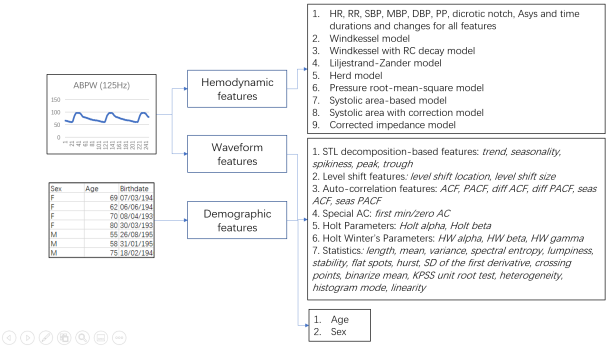

Fig. 2. Feature engineering from ABP waveform and demographic records.

A. Traditional ABPW models for feature engineering

The beat-to-beat HR, BP, DBP, and MAP from arterial waveforms are the basic hemodynamic parameters. Also, PP (Pulse Pressure), dicrotic notch, Asys (the area under the curve of the systolic part of the arterial pressure) [4], and their time durations and changes also reflect the hemodynamic

status [17]. Besides, traditional ABPW algorithms model the arteries as a pneumatic air chamber and transfer the blood pressure into the power or volume values, shown in Table I [13].

Thus, we fuse the above hemodynamic parameters with traditional ABPW models' domain knowledge as hemodynamic features, shown in Fig. 2.

1) Noise and abnormal process: In practice, The ABP waveform data has noise and/or abnormalities, as shown in Fig. 3. Noise results in extracting the wrong heart beat periodic intervals. The procedure summarized in Algorithm 1 is to filter out the noise based on RR interval normal/abnormal values.

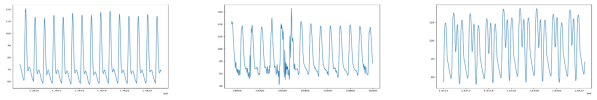

(a) Normal waveform (b) Waveform with noise (c) Abnormal waveform

Fig. 3. Noise and abnormal waveform.

Algorithm 1: adjust peak_list with RR value difference

Input: peak_list and RR_list to be adjusted
Output: peak_list_adjust

write the value of peak_list[0] *into peak_list_adjust*;
mean ← RR_mean;
for $i \leftarrow 0$ **to** $\text{len}\,(\text{RR}) - 1$ **do**
    $a \leftarrow$ RR[i];
    if $a - \text{mean} < const$ **then**
        while $a = a + \text{RR[i + 1]} < \text{const}$ **do**
            $a = a + \text{RR[i]}$;
            peak_list_adjust[i] ← peak_list[i+1];
    if $a - \text{mean} > \text{const}$ **then**
        rr_m ← $\text{round}\,(\text{a/mean})$;
        rr_interval ← a/rr_m;
        p_interval ← rr_interval/(1000/freq_ABPW);
        p_d ← peak_list_adjust[i-1];
        for rr_i ← 0 **to** rr_m-1 **do**
            peak_list_adjust[i] ← p_d + p_interval;
Return peak_list_adjust;

B. Waveform features

In this study, 39 waveform features are abstracted from 10s waveform and incorporated into machine learning models as inputs, including: Seasonal and Trend decomposition, the strength of seasonality, the strength of trend, spikiness, linearity, amount of level shift, presence of flat segments, the Auto-Correlation Function (ACF), the Partial Auto-Correlation Function (PACF), Hurst exponent, the Auto-Regressive Conditional Heteroskedasticity (ARCH) statistic, etc.

C. Demographic information

The study includes 227 patients of either sex, aged from 37-90 years in ICU. Two kinds of demographic information are taken into consideration: age and sex. The characteristics of the patients are displayed in Table II. The training and testing sets have the similar statistic distributions among patients.

IV. Model Training and Result Analysis

A. Model training and testing

Machine learning methods have been already widely used to analyze various physiological data and waveform signals [27], [28]. We extract the waveform-related and hemodynamic-related features from arterial pulse waveform signals and input these features combined with patients' demographic information into the machine learning models.

We divide the training, validation and test dataset as 8:1:1 (training size: $2,226$; validation size: 247; test size: 268) and use 10-fold cross-validation to evaluate 19 machine learning models categorized into 6 types: linear regressor, linear ridge regressor, and linear lasso regressor belong to the linear regression model; decision tree regressor and extra tree regressor belong to the tree model; random forest regressor, HGB regressor, GBR regressor, ABR regressor, bagging regressor, XGBoost regressor, LightGBM regressor, and CatBoost regressor belong to ensemble model (specifically, the XGBoost regressor, LightGBM regressor, and CatBoost regressor use the gradient boosting method, which is widely used and has good performance in the clinical domain); Gaussian regressor, Bayesian ridge regressor, and ARD regressor belong to Bayesian model; neural network regressor, KNN regressor, and SVM regressor belong to other models.

B. Result analysis

We evaluate all the above models and choose one or more representatives from each type for the final result comparison.

1) Distribution and box plot: Fig. 4 shows the distribution or spread out between the model predicting results and TCO. Most CO values are between 4 to 7 L/min and the distributions are similar to the measured TCO. Machine learning and feature engineering have similar distribution characteristics.

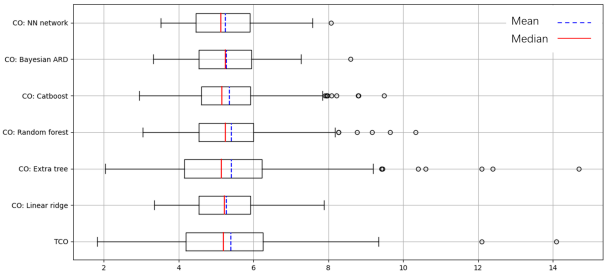

Fig. 4. Disctribution and boxplot.

2) Regression evaluation: Estimating CO is a regression issue to predict the CO value of the last timestamp in the ABPW time window. In this study, seven regression evaluation metrics are used to summarize the predictive skills, shown in Table III. From the results, Random Forest, CatBoost, and XGBoost can be seen as the top three performing models.

3) Meta-analysis of four graphic: In the hemodynamic domain, especially CO prediction task, the meta-analysis describe the relationship between the TCO and predicted CO [3]. The Meta-analyses summarised results from seven representative models are shown in Table IV and Fig. 5∼Fig. 8.

TABLE I
ALGORITHMS TO ESTIMATE CO FROM ABP WAVEFORMS

Algorithm name	**Algorithm description**
Mean Pressure [18]	$k\times$ MAP
Windkessel (1904) [19]	$k \times (SBP - DBP) \times$ HR
Windkessel with RC decay (1976) [20]	$k \times \frac{MAP}{T} \times \ln \frac{SBP}{DBP} \times$ HR
Liljestrand-Zander (1928) [21]	$k \times \frac{SBP-DBP}{SBP+DBP} \times$ HR
Herd (1966) [22]	$k \times (MAP - DBP) \times$ HR
Pressure root-mean-square (2002) [23]	$k \times \sqrt{\int_T (ABP(t) - MAP)^2 \mathrm{d}t} \times$ HR
Systolic area (1959) [24]	$k \times \int_{\mathrm{sys}} ABP(\mathrm{d}t) \times$ HR
Systolic area with Kouchoukos correction (1970) [25]	$k \times \int_{sys} ABP(\mathrm{d}t) \times (1 + \frac{T_{sys}}{T_{dia}}) \times$ HR
Corrected impedance (1983) [26]	$k \times (163 + HR - 0.48 \times MAP) \times \int_{\mathrm{sys}} ABP(\mathrm{d}t) \times$ HR

TABLE II
PATIENT CHARACTERISTICS FOR TRAINING AND TESTING SET

	Training set (n=2473, p=226)	**Test set** (n=268,p=121)	**Total set** (n=2741,p=227)
Demographics			
Age (years)	37 - 90 70 [62-77] 69.8±11.6	37 - 90 72 [61-77] 68.7±13.0	37 - 90 70 [62-77] 69.7±11.8
Sex (male)	62.2%	63.3%	62.3%
Hemodynamic characteristics			
HR	0 - 138.3 86.2 [77.5-93.1] 85.4±13.3	0 - 153.7 86.1 [76.5-94.7] 85.7±16.5	0 - 153.7 86.2 [77.5-93.3] 85.4±13.6
ABP Sys (SBP)	0 - 196.8 113.6 [102.2-126.7] 110.6±32.0	0 - 190.3 113.7 [102.2-126.8] 111.0±34.0	0 - 196.8 113.6 [102.2-126.7] 110.6±32.2
ABP Dias (DBP)	0 - 102.9 55.1 [49.2-62] 53.5±15.7	0 - 94.6 54.8 [48.7-61.8] 53.3±16.4	0 - 102.9 55 [49.2-62] 53.5±15.8
ABP Mean (MAP)	-7.8 - 291 75.8 [68.4-83.9] 76.1±20.5	0 - 243.1 75.2 [67.9-83.7] 76.3±21.8	-7.8 - 291 75.8 [68.4-83.8] 76.1±20.6
CO (TCO)	1.55 - 19.1 4.91 [4.11-6.12] 5.2±1.7	1.82 - 14.1 5.2 [4.2-6.3] 5.4±1.7	1.55 - 19.1 4.94 [4.11-6.13] 5.2±1.7

n: values are expressed as the number of segmentations.
p: values are expressed as the number of patients.
Age: values are expressed as min-max, median [quartile 25% - quartile 75%], mean±std.
Sex: values are expressed as percent.
HR, ABP Sys, ABP Dias, ABP Mean, CO as measured by monitoring.

TABLE III
REGRESSION EVALUATION RESULTS

Regression results	**Machine Learning Models**						
	Linear ridge	*Extra tree*	*Random forest*	*CatBoost*	*XGBoost*	*Bayesian ARD*	*NN Network*
MSE	1.967	3.460	**1.421**	1.468	1.513	1.962	1.940
RMSE	1.403	1.860	**1.192**	1.211	1.230	1.401	1.393
MSLE	0.045	0.073	**0.032**	0.033	0.034	0.045	0.044
MAE	1.057	1.334	0.945	**0.931**	0.957	1.062	1.047
MAPE	20.739	25.294	18.424	**18.057**	18.453	20.899	20.494
MedAE	0.865	0.965	0.779	0.777	**0.765**	0.869	0.852
R2 score	0.296	-0.238	**0.492**	0.475	0.459	0.298	0.306

The scatter plot and fitting curves represent the agreement or consistency between the TCO and predicted CO. The data points lie within close proximity to the line of identity x = y for there to be a good agreement, shown in Fig. 5.

Altman-Bland plot with Bias, LOA (Limits of Agreement), and PE (Percentage Error) [29], is a way to evaluate a bias between the mean difference and an agreement interval, shown in Fig. 6. The Random Forest model is within a bias of -0.01 L/min, the LOA of [-2.35 to 2.32] L/min and the PE of 39.44 %, and it performs best, compared to other machine learning models, while it can still not reach a clinically good agreement range (PE$\leq$30%) [3], [14].

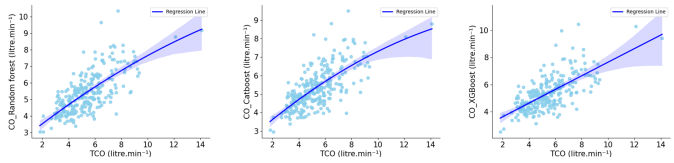

Fig. 5. Scatter plots.

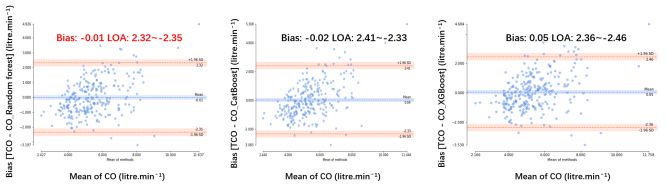

Fig. 6. Bland-Altman plot.

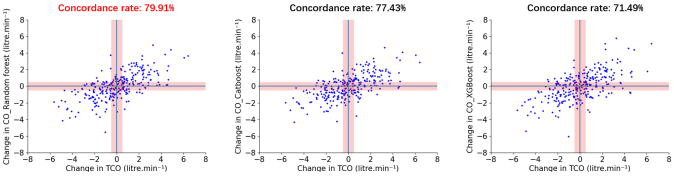

Fig. 7. Four-quandrant plot.

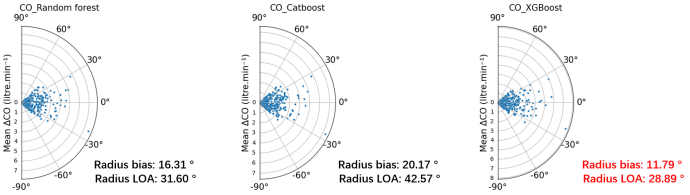

Fig. 8. Polar plot.

Besides the absolute accuracy and precision, it is also important to assess the ability to track changes in CO. The Four-quadrant plot (with concordance rate given in Fig. 7) and the Polar plot (with the angular bias and radial LOA given in Fig. 8) [14] are utilized for trending capabilities analysis. From the Four-quadrant plot results, the concordance rate of the Random forest model is 79.91%, and polar plot analysis results

in an angular bias of 16.31° with radial LOA of ±31.60°. The XGBoost models' radial LOA is ±28.89°, within the clinically acceptable trending tracking ability for CO changes (radial LOA$\leq \pm 30°$) [3], [14].

Through the above results, Random Forest, CatBoost, and XGBoost perform best among other tested models for agreement and trending ability. And XGBoost shows a good clinical acceptable trending ability when predicting CO values.

C. Explanations and interpretation

1) Feature contribution analysis: We utilize three different sets of features: hemodynamic features, waveform features, and demographic features. We combine and separate feature sets to re-train and test with Random forest model. The results are listed in Table V: through the combination of all three different feature sets, our model provided improved performance in estimating the CO values.

2) Feature importance: For each feature, we calculated their importance within the tree-based models as their performance was more accurate than the other tested ones. In Table VI, we list details of the top 10 features according to their F-scores for Random forest, CatBoost, and XGBoost models. From the importance analysis, demographic features (age and sex) are the two most important factors in the results while hemodynamic features and waveform features both contribute to the models as well.

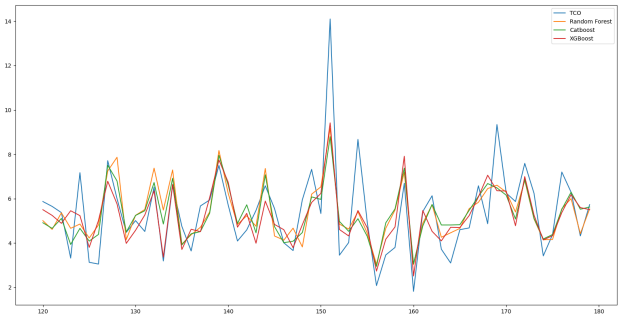

Fig. 9. Representative plot for interpretation of the tracking CO ability. In this plot, x-axis represents the time while the y-axis is for CO values.

3) Representative plot and tracking ability: The representative plot in Fig. 9 shows the tracking of CO trends of our models and the gold standard provided by test datasets. The proposed models (orange, green, or red) shows a similar trend to the golden standard CO (blue). It is noteworthy that when TCO changes rapidly, our model can only track the change direction, not to the same extent.

V. Discussion

Based on result analysis, we identified future directions:

- Patient demographic information: we only introduce age and sex due to the dataset limits. From the feature importance analysis, the patient demographic information plays an important role in predicting CO. Our clinical knowledge tells us that the patient body mass index affects the vascular resistance and hemodynamics. We plan to add more demographic information, especially patients' weights and heights into the feature vector to improve the performance of the presented model.
- As for feature engineering, features extracted based on traditional hemodynamic models need an accurate separation of the RR interval and dicrotic notch periods. When ABP waveforms are abnormal or noisy under ICU or severe operations, it become difficult to process. For such cases, we filter the noise by taking into account the normal and/or mean RR. However, performance of filtering noise is still limited. We will use deep learning models to extract the ABP waveform and automatically process the abnormal situation.

VI. Conclusion

In this study, we proposed the feature engineering and machine learning methods to predict CO from the ABP waveform. Features include information based on traditional hemodynamic models and waveform or time series features. Putting patient demographics together, we input all three kinds of features into different machine learning models. We also provided our benchmarking results for several machine learning models on public MIMIC-II datasets and evaluated them by boxplot, regression evaluation metrics, and meta-analysis of four graphic plots. As evidenced by our results, the ensemble models (Random Forest, CatBoost and XGBoost) show good predicting results in all evaluation indicators.

Future work would not only include more demographic information but also use deep learning models to improve the feature extraction in order to overcome the difficulties imposed by severely abnormal signals.

References

[1] M. Cecconi, D. De Backer, M. Antonelli, R. Beale, J. Bakker, C. Hofer, R. Jaeschke, A. Mebazaa, M. R. Pinsky, J. L. Teboul *et al.*, "Consensus on circulatory shock and hemodynamic monitoring. task force of the european society of intensive care medicine," *Intensive care medicine*, vol. 40, no. 12, pp. 1795–1815, 2014.

[2] B. Kolb and V. Kapoor, "Cardiac output measurement," *Anaesthesia & Intensive Care Medicine*, vol. 20, no. 3, pp. 193–201, 2019.

[3] L. A. H. Critchley, "Minimally invasive cardiac output monitoring in the year 2012," *Artery Bypass*, 2013.

[4] S. A. Esper and M. R. Pinsky, "Arterial waveform analysis," *Best Practice & Research Clinical Anaesthesiology*, vol. 28, no. 4, pp. 363–380, 2014.

[5] O. Frank, "The basic shape of the arterial pulse. first treatise: mathematical analysis," *Journal of molecular and cellular cardiology*, vol. 22, no. 3, pp. 255–277, 1990.

[6] A. Rhodes and R. Sunderland, "Arterial pulse power analysis: the lidco plus system," in *Functional hemodynamic monitoring*. Springer, 2005, pp. 183–192.

[7] J. Mayer, J. Boldt, T. Schöllhorn, K. Röhm, A. Mengistu, and S. Suttner, "Semi-invasive monitoring of cardiac output by a new device using arterial pressure waveform analysis: a comparison with intermittent pulmonary artery thermodilution in patients undergoing cardiac surgery," *British journal of anaesthesia*, vol. 98, no. 2, pp. 176–182, 2007.

[8] W. Jin, "Cardiovascular function assessment using computational blood flow modelling and machine learning," Ph.D. dissertation, King's College London, 2021.

[9] H.-L. Yang, H.-C. Lee, C.-W. Jung, and M.-S. Kim, "A deep learning method for intraoperative age-agnostic and disease-specific cardiac output monitoring from arterial blood pressure," in *2020 IEEE 20th International Conference on Bioinformatics and Bioengineering (BIBE)*. IEEE, 2020, pp. 662–666.

TABLE IV
META-ANALYSIS RESULTS

Method	Linear regression			Bland-Altman plot				Four-quadrant plot	Polar plot	
	MSE	MAE	R2	Bias (L/min)	Lower LOA (L/min)	Upper LOA (L/min)	PE (%)	Concordance rate (%)	Angular bias (°)	Radial LOA (°)
Random forest	**1.421**	**0.945**	**0.492**	**−0.01**	**−2.35**	**2.32**	**39.44**	**79.91**	16.31	**31.60**
CatBoost	**1.468**	**0.931**	**0.475**	**−0.02**	**−2.33**	**2.41**	**40.35**	**77.43**	20.17	42.57
XGBoost	1.513	0.957	0.459	0.05	-2.36	2.46	42.10	71.49	**11.79**	**28.89**
Linear ridge	1.967	1.057	0.296	0.12	-2.62	2.86	48.39	72.89	**15.81**	37.15
Extra tree	3.460	1.334	-0.238	**−0.02**	-3.67	3.62	61.41	65.56	21.63	41.90
Bayesian ARD	1.962	1.062	0.298	0.12	-2.62	2.86	48.64	72.97	18.33	37.33
NN Network	1.940	1.047	0.306	0.14	-2.58	2.86	48.66	72.65	21.91	43.13

TABLE V
FEATURE CONTRIBUTION ANALYSIS (MODEL: RANDOM FOREST)

Feature selection	MSE	R2	Concordance rate	Bias	LOA	Angular bias	Radial LOA
Hemodynamic	2.823	-0.010	56.50%	0.03	-3.27∼+3.32	16.30°	±41.16°
Waveform	2.178	0.221	63.37%	0.07	-2.82∼+2.96	19.23°	±38.70°
Demographic	1.787	0.361	71.08%	0.04	-2.58∼+2.66	25.10°	±45°
Hemodynamic & Waveform	2.230	0.202	64.34%	0.06	-2.86∼+2.98	19.39°	±41.19°
Hemodynamic & Demographic	1.609	0.424	77.20%	-0.02	-2.51∼+2.47	21.15°	±40.73°
Waveform & Demographic	1.570	0.439	75.20%	**-0.01**	-2.47∼+2.44	17.10°	±41.85°
Hemodynamic, Waveform & Demographic	**1.421**	**0.492**	**79.91%**	**0.01**	**-2.35∼+2.32**	**16.31°**	**±31.60°**

[10] Y.-J. Moon, H. S. Moon, D.-S. Kim, J.-M. Kim, J.-K. Lee, W.-H. Shim, S.-H. Kim, G.-S. Hwang, and J.-S. Choi, "Deep learning-based stroke volume estimation outperforms conventional arterial contour method in patients with hemodynamic instability," *Journal of clinical medicine*, vol. 8, no. 9, p. 1419, 2019.

[11] H.-M. Kwon, W.-Y. Seo, J.-M. Kim, W.-H. Shim, S.-H. Kim, and G.-S. Hwang, "Estimation of stroke volume variance from arterial blood pressure: Using a 1-d convolutional neural network," *Sensors*, vol. 21, no. 15, p. 5130, 2021.

[12] J. Sun, A. Reisner, M. Saeed, and R. Mark, "Estimating cardiac output from arterial blood pressurewaveforms: a critical evaluation using the mimic ii database," in *Computers in Cardiology, 2005*. IEEE, 2005, pp. 295–298.

[13] J. Zhang, L. Critchley, and L. Huang, "Five algorithms that calculate cardiac output from the arterial waveform: a comparison with doppler ultrasound," *British Journal of Anaesthesia*, vol. 115, no. 3, pp. 392–402, 2015.

[14] L. A. Critchley, X. X. Yang, and A. Lee, "Assessment of trending ability of cardiac output monitors by polar plot methodology," *Journal of cardiothoracic and vascular anesthesia*, vol. 25, no. 3, pp. 536–546, 2011.

[15] M. Saeed, M. Villarroel, A. T. Reisner, G. Clifford, L.-W. Lehman, G. Moody, T. Heldt, T. H. Kyaw, B. Moody, and R. G. Mark, "Multiparameter intelligent monitoring in intensive care ii (mimic-ii): a public-access intensive care unit database," *Critical care medicine*, vol. 39, no. 5, p. 952, 2011.

[16] M. Saeed, C. Lieu, G. Raber, and R. G. Mark, "Mimic ii: a massive temporal icu patient database to support research in intelligent patient monitoring," in *Computers in cardiology*. IEEE, 2002, pp. 641–644.

[17] M. Nirmalan and P. M. Dark, "Broader applications of arterial pressure wave form analysis," *Continuing Education in Anaesthesia, Critical Care & Pain*, vol. 14, no. 6, pp. 285–290, 2014.

[18] J. X. Sun, "Cardiac output estimation using arterial blood pressure waveforms," Ph.D. dissertation, Massachusetts Institute of Technology, 2006.

[19] J. Erlanger, "An experimental study of blood-pressure and of pulse-pressure in man," *Bull Johns Hopkins Hosp*, vol. 12, pp. 145–378, 1904.

[20] T. B. Watt Jr and C. S. Burrus, "Arterial pressure contour analysis for estimating human vascular properties," *Journal of applied physiology*, vol. 40, no. 2, pp. 171–176, 1976.

[21] G. Liljestrand and E. Zander, "Vergleichende bestimmungen des minutenvolumens des herzens beim menschen mittels der stickoxydulmethode und durch blutdruckmessung," *Zeitschrift für die gesamte experimentelle Medizin*, vol. 59, no. 1, pp. 105–122, 1928.

[22] J. A. Herd, N. R. Leclair, and W. Simon, "Arterial pressure pulse contours during hemorrhage in anesthetized dogs," *Journal of Applied Physiology*, vol. 21, no. 6, pp. 1864–1868, 1966.

[23] M. M. Jonas and S. J. Tanser, "Lithium dilution measurement of cardiac output and arterial pulse waveform analysis: an indicator dilution calibrated beat-by-beat system for continuous estimation of cardiac output," *Current opinion in critical care*, vol. 8, no. 3, pp. 257–261, 2002.

[24] W. B. Jones, L. L. Hefner, W. Bancroft, W. Klip *et al.*, "Velocity of blood flow and stroke volume obtained from the pressure pulse," *The Journal of clinical investigation*, vol. 38, no. 11, pp. 2087–2090, 1959.

[25] N. T. Kouchoukos, L. C. Sheppard, and D. A. McDONALD, "Estimation of stroke volume in the dog by a pulse contour method," *Circulation Research*, vol. 26, no. 5, pp. 611–623, 1970.

[26] K. Wesseling, "A simple device for the continuous measurement of cardiac output. its model basis and experimental varification," *Adv. Cardiovasc. Phys.*, vol. 5, pp. 16–52, 1983.

[27] F. Hatib, Z. Jian, S. Buddi, C. Lee, J. Settels, K. Sibert, J. Rinehart, and M. Cannesson, "Machine-learning algorithm to predict hypotension based on high-fidelity arterial pressure waveform analysis," *Anesthesiology*, vol. 129, no. 4, pp. 663–674, 2018.

[28] X. Zhao, K. Liao, W. Wang, J. Xu, and L. Meng, "Can a deep learning model based on intraoperative time-series monitoring data predict post-hysterectomy quality of recovery?" *Perioperative Medicine*, vol. 10, no. 1, pp. 1–12, 2021.

[29] D. Giavarina, "Understanding bland altman analysis," *Biochemia medica*, vol. 25, no. 2, pp. 141–151, 2015.

TABLE VI
TOP 10 IMPORTANCE FEATURES FOR THE BEST PERFORMING MODELS

Random Forest				CatBoost				XGBoost			
Features			F-scores	Features			F-scores	Features			F-scores
Demographic		age	0.20805343	Demographic		age	17.11552	Demographic		age	0.14337
Demographic		sex	0.13356746	Demographic		sex	9.863423	Demographic		sex	0.099373
Waveform	Statistics	unitroot_kpss	0.03719396	Waveform	Statistics	entropy	2.687641	Hemodynamic	RR	RR_neg	0.025792
Waveform	Auto-correlation	diff1y_acf5	0.0262601	Waveform	Statistics	unitroot_kpss	2.646477	Hemodynamic	Systolic area	SV_sa	0.024887
Waveform features	Statistics	entropy	0.02274849	Waveform	Statistics	binarize_mean	2.427249	Waveform	Special AC	firstmin_ac	0.024814
Waveform	Auto-correlation	seas_pacf1	0.02001269	Waveform	STL features	seasonality	2.198293	Waveform	Auto-correlation	diff1y_acf5	0.022681
Hemodynamic	Liljestrand-Zander	CO_Lilj	0.01886984	Waveform	STL features	linearity	1.909788	Waveform	Level shift features	level_shift_size	0.02002
Waveform	STL features	trend	0.01832945	Waveform	Auto-correlation	diff2y_pacf5	1.894529	Waveform	Auto-correlation	diff2y_pacf5	0.019285
Waveform	STL features	seasonality	0.01793782	Waveform	Auto-correlation	diff1y_acf5	1.818168	Waveform	Auto-correlation	diff2y_acf1	0.01851
Hemodynamic	RR	RR_neg	0.01551073	Waveform	Auto-correlation	diff1y_acf1	1.692284	Waveform	Auto-correlation	y_acf5	0.01777